**Conference paper**

Jasper Wattjes, Baptiste Schindler, Stéphane Trombotto, Laurent David, Bruno M. Moerschbacher and Isabelle Compagnon*

# Discrimination of patterns of *N*-acetylation in chitooligosaccharides by gas phase IR spectroscopy integrated to mass spectrometry

DOI 10.1515/pac-2017-0110

**Abstract:** We propose a novel, bi-dimensional analysis of partially *N*-acetylated chitosan oligosaccharides based on gas phase Infra-Red spectroscopy integrated to mass spectrometry (MS). By providing simultaneously MS and IR fingerprints, this approach combines the advantages of MS with the refined structural detail offered by gas phase spectroscopy and provides robust signatures for the rapid discrimination of the patterns of *N*-acetylation. Four mono-*N*-deacetylated and two doubly-*N*-deacetylated chitosan tetramer standards with well-defined patterns of acetylation were produced and analyzed by IR integrated to MS. We show that each sequence displays a unique combination of MS and IR fingerprints, thus offering a rapid diagnostic for the pattern of acetylation without the need for reducing end labeling.

**Keywords:** carbohydrates; chitosans; experimental methods; glycomics; ICS-28; mass spectrometry; spectroscopy.

## Introduction

Functional biopolymers and oligomers such as chitosans are still poorly understood when it comes to structure-function relationships including their biological modes of action. However, these biopolymers have shown great potential to be used in a broad range of sustainable applications [1]. The lack of understanding structure-function relationships is mainly caused by the varying chemical structure and heterogeneity of these materials [2]. To overcome this problem, innovative and controlled processes that can deliver well-defined products are necessary. To that end sophisticated analytical methods are in turn needed to allow structures elucidation and characterization [3, 4].

Chitosans are linear co-polymers and oligomers consisting of β-(1→4) linked 2-acetamido- 2-deoxy-D-glucopyranosyl (GlcNAc, referred to as A) and 2-amino-2-deoxy-D-glucopyranosyl (GlcN, referred to as D) units. The free amino groups of GlcN (pKa 6.5) are positively charged at slightly acidic pH and are responsible for the unique polycationic character of chitosans. This polycationic character is maybe the most important

**Article note:** A collection of invited papers based on presentations at the XXVIII International Carbohydrate Symposium (ICS-28), New Orleans, July 17–21 2016.

***Corresponding author: Isabelle Compagnon,** Institut Lumière Matière, Univ Lyon, Université Claude Bernard Lyon 1, CNRS, F-69622 Villeurbanne, France; and Institut Universitaire de France IUF, 103 Blvd St Michel, 75005 Paris, France, e-mail: isabelle.compagnon@univ-lyon1.fr
**Jasper Wattjes and Bruno M. Moerschbacher:** Institut für Biologie und Biotechnologie der Pflanzen, Westfälische Wilhelms-Universität Münster, Schlossplatz 8, 48143 Münster, Germany
**Baptiste Schindler:** Institut Lumière Matière, Univ Lyon, Université Claude Bernard Lyon 1, CNRS, F-69622 Villeurbanne, France
**Stéphane Trombotto and Laurent David:** Laboratoire Ingénierie des Matériaux Polymères (IMP), CNRS UMR 5223, Univ. Lyon, Université Claude Bernard Lyon 1, 15 bd A. Latarjet, 69622 Villeurbanne, France

© 2017 IUPAC & De Gruyter. This work is licensed under a Creative Commons Attribution-NonCommercial-NoDerivatives 4.0 International License. For more information, please visit: http://creativecommons.org/licenses/by-nc-nd/4.0/

reason for the diverse application fields of chitosans such as wound healing, drug delivery, crop protection, waste water treatment or antimicrobial ingredients [5–8]. The heterogenic family of chitosan oligomers and polymers can be characterized by their degree of polymerization (DP), their fraction of acetylation ($F_A$) and their pattern of *N*-acetylation (PA) [9]. The bioactivity of chitosan polymers and oligomers was already shown to be strongly dependent on DP and $F_A$ [2, 10–13]. In addition, the PA has been proposed to influence bioactivity [14] since the distribution of acetyl groups will influence the interaction with specific receptors or the susceptibility of chitosans as substrate to pattern-specific chitosanolytic enzymes that are present in biological systems [15, 16]. However, chitosan oligomers on the market today are mainly produced by two approaches: (i) by depolymerization of chitin and chitosan polymers under the action of chemical reagents, enzymes and high energy impact [17, 18]; and (ii) by partial *N*-acetylation of glucosamine oligomers [19, 20] These processes yield highly heterogeneous mixtures that strongly depend on the chemical and physical characteristics of the starting material and on technical production parameters. Structurally well-defined chitooligosaccharides (COS) can be obtained from monosaccharide building blocks by total chemical synthesis [21]. Approaches for the synthesis of COS and congeners have recently been reviewed by Yang and Yu [22]. However, these techniques require sophisticated amino protection-deprotection manipulations.

As an alternative, the biotechnological production of well-defined chitosans using specific chitin and chitosan modifying enzymes has emerged as a promising possibility. Partially *N*-acetylated chitooligosaccharides (paCOS) with a non-random PA can be produced using enzymatic depolymerization or deacetylation [23–25]. To investigate their structure-function relationships, the PA of these paCOS needs to be verified and investigated by appropriate analytical methods.

So far paCOS were investigated using nuclear magnetic resonance spectroscopy (NMR) or mass spectrometry (MS) [26, 27]. A major drawback of NMR is the need of large amounts of pure sample. Besides, sequences of paCOS with different PA cannot be fully elucidated [28]. In contrast, MS analysis applies to small amounts of sample, does not require thorough purification, and readily resolves both the degrees of polymerization and the $F_A$, which is appealing. To further discriminate between isomeric sequences, labeling techniques have been used to mark the reducing end [29, 30]. However, these techniques had several drawbacks especially regarding purification issues after the labeling process.

To further exploit the performance of MS analysis, the authors have proposed two sequencing strategies to elucidate the PA in chitosan oligomers. Both approaches were based on the identification of the reducing end, combined with fragmentation of the oligosaccharide by multistage MS ($MS^n$). The identification of the reducing end was done either by $H_2{}^{18}O$ labeling [3], or by Infrared spectroscopy integrated to MS [4], without requiring any chemical modification.

Following these previous reports on chitosan sequencing, we propose an alternative approach for the rapid identification of partially *N*-acetylated chitosan oligomers, based on gas phase IR spectroscopy integrated to MS. By providing simultaneously MS and IR fingerprints, this approach combines the advantages of MS with the refined structural detail offered by gas phase IR spectroscopy. We show that chitosan tetramers standards of well-defined DP, degree of acetylation and pattern of acetylation have a unique bi-dimensional MS-IR signature, and we discuss the potential of this original combination of MS and spectroscopic reference data for the rapid discrimination of patterns of *N*-acetylation in chitosan oligomers.

# Materials and methods

## Enzyme production

All enzymes were produced heterologously in *Escherichia coli* expression systems and afterwards purified using a Fast protein liquid chromatography (FPLC) system (Äktaprime™ plus; GE Healthcare Life Sciences, Uppsala, Sweden) equipped with a Strep-Tactin Superflow Plus Matrix column (1 bed volume, Qiagen, Hilden, Germany) as previously described [16, 25, 31].

## Size exclusion chromatography (SEC)

To purify GlcNAc tetramer and to remove residual salts and protein after enzymatic treatments, a SECcurity GPC System (PSS Polymer Standards Service, Mainz, Germany) with an Agilent 1200 series refractive index detector (Agilent Technologies, Santa Clara, CA, USA) was used. Before injection, samples were filtered using a 0.22 μm syringe filter. Separation was achieved using a HiLoad™ Superdex™ 30 prep grade column (Pharmacia, Uppsala, Sweden) at a flow rate of 0.3 mL/min of 0.15 M ammonium acetate buffer pH 4.5. Data was recorded using the WinGPC UniChrom software (PSS Polymer Standards Service, Mainz, Germany). To remove ammonium acetate buffer, samples were subjected to several washing and freeze-drying steps. Purity of samples was evaluated with UHPLC-ESI-MS.

## Production of specific chitosan oligomers

The six sequences shown in Scheme 1 were produced as follows: GlcNAc tetramer (AAAA) was purified as a side product from GlcNAc pentamer originating from large scale fermentation [25] using size exclusion chromatography (SEC). Specific tetramers DAAA, ADAA, AADA, DDAA and AADD were produced as previously described [16, 25, 31] by treating GlcNAc tetramer with four different enzymes, NodB, COD, PesCDA and PgtCDA, respectively. The treatment was carried out in 0.15 M ammonium acetate buffer (pH 4.5). The tetramer AADD was further purified using preparative hydrophilic interaction liquid chromatography (HILIC). The tetramer with the sequence AAAD was kindly provided by Dr. Antonio Segade Rodríguez, Enantia S.L., Barcelona, Spain.

## Hydrophilic liquid interaction chromatography (HILIC)

To further purify AADD tetramer and remove residual AADA contamination due to incomplete PgtCDA reaction, preparative HILIC was carried out. The tetramers were separated using a method based on Cord-Landwehr et al. [3]. To this end, a Prominence LC-20AD HPLC system (Shimadzu Corporation, Tokyo, Japan) equipped with an XBridge® BEH OBD™ PREP column (5 μm, 250 × 10 mm; Waters Corporation, Milford, MA, USA), a flow rate of 2 mL/min as well as 50 °C oven temperature were used. We performed an LC run over 60 min with the following gradient elution profile for sample separation: 0–10 min, isocratic 100 % A (80:20 ACN/$H_2O$ with 10 mM $NH_4HCO_2$ and 0.1 % (v/v) HCOOH); 10–50 min, linear from 0 % to 75 % (v/v) B (20:80 ACN/$H_2O$ with 10 mM $NH_4HCO_2$ and 0.1 % (v/v) HCOOH); re-equilibration: 50–54 min, linear from 20 % (v/v) to 100 % A; 54–60 min, isocratic 100 % A. Samples were collected based on the signal of an SPD-20A UV-VIS detector (Shimadzu Corporation, Tokyo, Japan) operating at 210 nm. After separation, remaining solvents were evaporated and the sample was freeze-dried.

## UHPLC-ESI-MS/MS

To validate the correct mass and *N*-acetylation pattern of all tetramers, UHPLC-ESI combined with MS was used as previously described [3].

## MS/MS analysis

A quadrupolar 3D ion trap (Thermofinnigan LCQ classic) equipped with an electrospray source was used for MS/MS analysis. Fifty micromolar solutions were prepared in $H_2O$:Methanol 50:50 and ionized in positive mode to produce protonated species. The singly charged mono *N*-deacetylated and doubly *N*-deacetylated tetramers tetramers were observed at m/z 789 and m/z 747, respectively. After isolation, they were resonantly

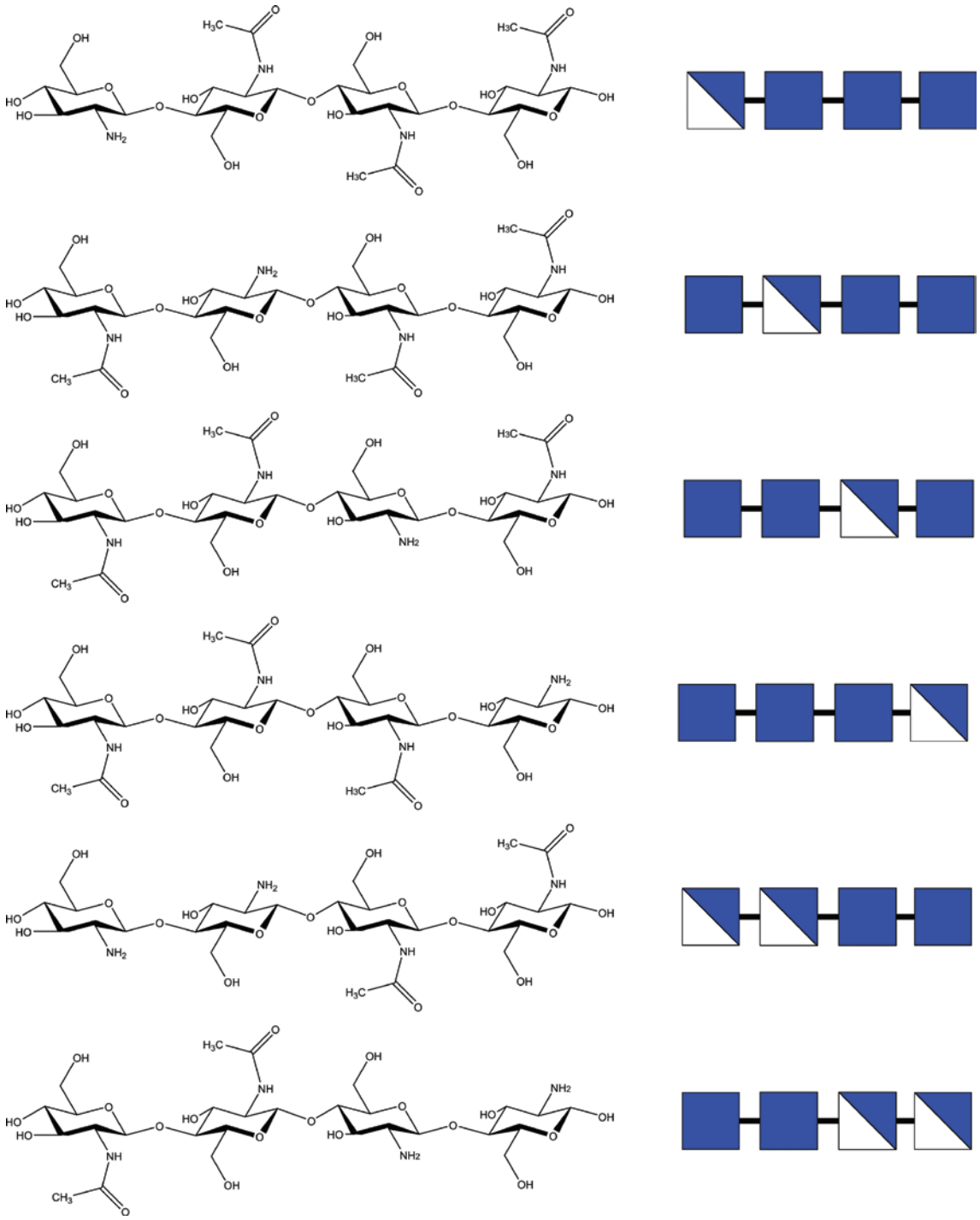

**Scheme 1:** Chemical structures of the investigated tetramers DAAA, ADAA, AADA, AAAD, DDAA and AADD (displayed from top to bottom). Carbohydrate symbol nomenclature from Ref. [32].

activated during 30 ms by collision (CID: collision induced dissociation) in the helium buffer present in the ion trap. First generation fragments are no longer resonant with the excitation but remain trapped and are promptly thermalized in the helium buffer, which prevents further fragmentation. In this MS/MS configuration, it is generally accepted that direct fragmentation pathways are promoted and sequential fragmentation pathways are hindered. The resulting MS/MS spectra are averaged 50 times.

### MS/IR analysis

Gas phase IR spectroscopy was enabled using the IRMPD spectroscopic scheme, as described in [4]. In short, the mass spectrometer was modified, as shown in Fig. 1. The trapping electrode was drilled and an IR-transparent window was installed to allow irradiation of the ion cloud by the laser beam produced by a YAG-pumped OPO/OPA system (LaserVision) tunable in the 3 μm region. Note that in traditional IR spectroscopy, the intensity of the incident and transmitted light are measured and the IR spectrum is retrieved using the Beer Lambert formula. Here this strategy cannot be employed, as the density of ions in the ion trap is too low (a few hundreds in a cubic millimeter) to detect a significant decreased of the intensity of the incident IR light. We use instead an "Action Spectroscopy" strategy, were the absorption of the light is detected via the observation of photoinduced fragmentation of the irradiated ions, as follows: mass-selected ions are isolated and irradiated for 700 ms, resulting in wavelength-dependent photofragmentation. The resulting photofragmentation spectrum is averaged 3 times and the photofragmentation yield is calculated using the following variation of the Beer-Lambert formula: $-\log(Ip/(Ip+\Sigma If))$, were $Ip$ is the intensity of the precursor ion and $If$ is the integrated intensity of the photofragments. In this spectroscopic scheme, the IR spectrum of the precursor ion is retrieved by monitoring the photofragmentation yield as a function of the wavelength.

## Results and discussion

The MS/MS and IR spectra of the four sequences of mono *N*-deacetylated tetramers and the two doubly *N*-deacetylated tetramers are shown in Figs. 2 and 3, respectively. The informative peaks are listed in Tables 1 and 2. A bold font is used to highlight the most intense fragments, and brackets indicate fragments that are present in extremely small amounts. Note that, according to the Domon and Costello nomenclature [33], the dissociation of a glycosidic bond may yield either or both of an intact saccharide subunit or a dehydrated subunit with a mass difference of 18. The two masses are reported in the tables for completeness, regardless of which fragment is actually seen in the mass spectra.

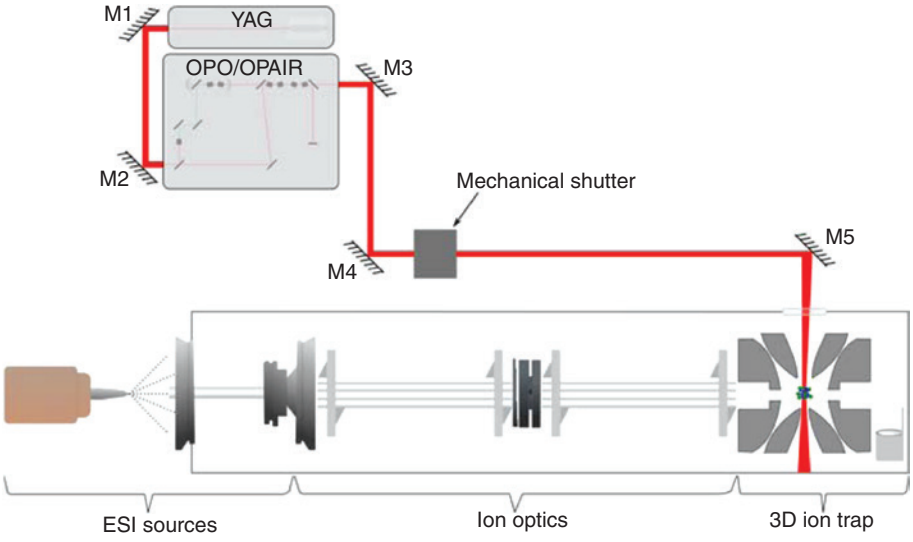


**Fig. 1:** Schematic of the mass spectrometer modified for integrating IR spectroscopy: a commercial LCQ Thermofinnigan mass spectrometer equipped with an ESI ion source was modified to allow laser irradiation of the ion cloud of mass selected analyses inside of the 3D ion trap. The IR laser beam produced by a YAG-pumped OPO/OPA laser system is guided towards the center of the ion trap, which was drilled for this purpose, using mirrors M3 to M5, and through an IR-transparent window. A mechanical shutter is used for the synchronization of the laser excitation with the period of isolation of the ions inside the trap.

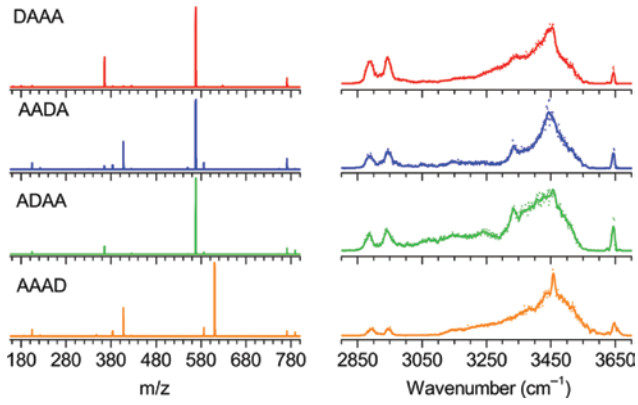


**Fig. 2:** MS/MS spectra (left) and gas phase IR spectra (right) of the four mono *N*-deacetylated tetramer sequences. Both MS/MS and IR spectra intensities are normalized on their most intense feature.

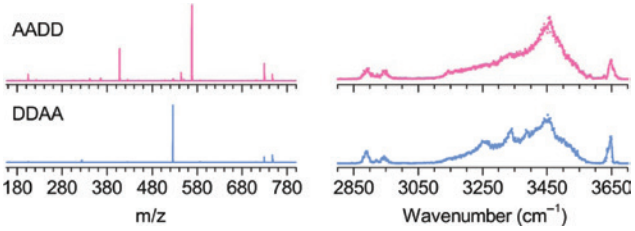


**Fig. 3:** MS/MS spectra (left) and gas phase IR spectra (right) of the two doubly *N*-deacetylated tetramer sequences. Both MS/MS and IR spectra intensities are normalized on their most intense feature.

**Table 1:** List of informative peaks found in the MS/MS spectra.

| Precursor | Pathway 1 fragmentation of a terminal GlcNAc | | Pathway 2 dissociation into two diholosides | | Pathway 3 fragmentation of a terminal GlcN | |
|---|---|---|---|---|---|---|
| 789 m/z | 568 or 586 m/z | 204 or 222 m/z | 365 or 383 m/z | 407 or 425 m/z | 610 or 628 m/z | 162 or 180 m/z |
| DAAA | **DAA** | A | DA | AA | (AAA) | (D) |
| AADA | **AAD** or **ADA** | A | DA | AA | – | – |
| ADAA | **ADA** or **DAA** | A | AD | AA | – | – |
| AAAD | AAD | A | AD | AA | **AAA** | D |

Tentative sequences are proposed for each fragment. The major MS/MS product is highlighted in bold font and pathways that are present but hardly detectable are in brakets. Pairs of masses in the header correspond to the two possible forms of each fragment (see text).

**Table 2:** List of informative peaks found in the MS/MS spectra.

| Precursor | Pathway 1 fragmentation of a terminal GlcNAc | | Pathway 2 dissociation into two diholosides | | Pathway 3 fragmentation of a terminal GlcN | |
|---|---|---|---|---|---|---|
| 747 m/z | 526 or 544 m/z | 204 or 222 m/z | 323 or 341 m/z | 407 or 425 m/z | 568 or 586 m/z | 162 or 180 m/z |
| AADD | ADD | A | DD | AA | **AAD** | D |
| DDAA | **DDA** | A | (DD) | (AA) | (DAA) | (D) |

Tentative sequences are proposed for each fragment. The major MS/MS product is highlighted in bold font and pathways that are present but hardly detectable are in brakets. Pairs of masses in the header correspond to the two possible forms of each fragment (see text).

The fragmentation patterns are rationalized as follows:

- Pathway 1 corresponds to the fragmentation of a terminal GlcNAc. The GlcNAc fragment ion at m/z 222 (or its dehydrated form at m/z 204), and the complementary trisaccharide fragment are diagnostic of this pathway. Here all six sequences display a GlcNAc unit in terminal position (either reducing end, non reducing end, or both ends). As a consequence, this pathway is always observed, and does not offer further information on the sequence. However, this pathway is dominant for sequences displaying a GlcNAc at the reducing end, which suggests that fragmentation at the reducing end is favored.
- Pathway 2 corresponds to the dissociation into two diholosides. The AA moiety at m/z 425 (or 407) and its complementary DA or DD (for mono- and doubly-*N*-deacetylated sequences, respectively) are diagnostic of this pathway. Again, this pathway is not directly informative, but the relative intensity of its diagnostic fragments is strongly sequence-dependant. General trends still need to be established however.
- Pathway 3 corresponds to the loss of a GlcN and is only possible when the sequence features a GlcN unit in terminal position. The GlcN fragment ion (m/z 180 or 162) and the complementary trisaccharide moiety are diagnostic of this pathway. We verify that the AADA and ADAA sequences which only have GlcNAc in terminal positions do not display this pathway. Among the remaining candidates, this pathway is dominant for AAAD and AADD, where GlcN is at the reducing end. This further indicates that fragmentation preferably takes place at the reducing end.

In complement to the MS/MS data, the gas phase IR spectra are recorded between 2800 and 3700 $cm^{-1}$. They display spectral features which are common to the six species: a narrow band at 3644 $cm^{-1}$ which corresponds to one or several free OH stretching vibration mode(s); an apex at 3550 $cm^{-1}$ and a partly unresolved band at 3337 $cm^{-1}$, which is typical of a combination of NH stretching modes and OH modes involved in intramolecular H-bonds; and two features at 2944 and 2888 $cm^{-1}$ in the CH stretching region. Despite these common features, the overall profiles are not identical, in particular in the 3000–3500 $cm^{-1}$ region.

This set of six tetramers clearly illustrates the limitations of one-dimensional analytical approaches and establishes the added value of our bi-dimensional MS/IR method. On one hand, MS alone is sufficient to resolve the DP and the degree of acetylation of a chitosan oligomer but bears no information on the pattern of acetylation. Even though some partial sequence information can be retrieved by MS/MS, fragmentation patterns may be ambiguous, as observed here for the sequences DAAA and ADAA, which yield almost identical MS/MS spectra. On the other hand, the IR signature is not strongly degree-of-acetylation-dependent, as seen here for AADD and DAAA which display nearly identical IR spectra, but is consistently pattern-of-acetylation-dependent within a series of isomers. Therefore, by measuring simultaneously the MS and IR fingerprints, it is possible to obtain a bi-dimensional signature which is sensitive altogether to the DP, the degree of acetylation and the pattern of acetylation. This is verified here with six tetramer sequences, which each display a unique set of MS and IR data.

## Conclusion

We have reported the first bi-dimensional MS/IR reference data for paCOS, to the best of our knowledge. With this approach, we add a spectroscopic dimension to MS analysis, which helps to resolve potential sequence ambiguities arising when the fragmentation patterns are not resolved, and without the need of labeling techniques.

The reference data established here for the DAAA, ADAA, AADA, AAAD, AADD and DDAA standards are essential to develop new synthetic or bio-synthetic pathways for the production of chitosan oligomers of controlled sequence, which remains a challenge. In this context, efficient test and trial strategies could now be implemented with the support of our rapid and robust method to discard unwanted products. In the future, reference data will also be produced for other degrees of polymerization and other degrees and patterns of *N*-acetylation.

More generally, although the IR analysis takes longer than a standard MS analysis (typically 20 min), both MS and IR fingerprints can be obtained on the same integrated instrument, and do not require any chemical modification of the analytes. We thus expect that this novel analytical approach has a strong potential for the rapid discrimination of paCOS isomers. Since MS is also an important tool to investigate enzymatic fingerprints of chitosan polymers, the addition of IR fingerprints as an additional dimension will help and contribute to investigate and characterize chitin and chitosan modifying enzymes.

In future studies, we will extend our investigations to higher and lower degrees of polymerization, in order to explore general trends. Indeed, establishing trends in the relationship between the pattern of acetylation and the MS/MS and MS/IR is crucial, as it will open the way to de novo analysis of the sequence of this class of molecules.

**Acknowledgements:** This work was supported by Institut Universitaire de France, the Fédération de Recherche André Marie Ampère and the Glycophysics Network (web: hwp://glyms.univ-lyon1.fr) funded by the French Agence Nationale de la Recherche (grant ANR-2015-MRSEI-0010).

## References

[1] M. Rinaudo. *Prog. Polym. Sci*. **31**, 603 (2006).
[2] N. E. El Gueddari, S. Kolkenbrock, A. Schaaf, N. Chilukoti, F. Brunel, C. Gorzelanny, S. Fehser, S. Chachra, F. Bernard, M. Nampally, T. Kalagara, P. Ihmor, B. M. Moerschbacher. *Adv. Chitin Sci*. **XIV**, 40 (2012).
[3] S. Cord-Landwehr, P. Ihmor, A. Niehues, H. Luftmann, B. M. Moerschbacher, M. Mormann. *Anal. Chem*. **89**, 2893 (2017).
[4] B. Schindler, G. Renois-Predelus, N. Bagdadi, S. Melizi, L. Barnes, S. Chambert, A.-R. Allouche, I. Compagnon. *Glycoconj. J*. (2016). doi: 10.1007/s10719-016-9741-8.
[5] T. Dai, M. Tanaka, Y.-Y. Huang, M. R. Hamblin. *Expert Rev. Anti. Infect. Ther*. **9**, 857 (2011).
[6] B. B. Aam, E. B. Heggset, A. L. Norberg, M. Sørlie, K. M. Vårum, V. G. H. Eijsink. *Mar. Drugs* **8**, 1482 (2010).
[7] S. N. Das, J. Madhuprakash, P. V. S. R. N. Sarma, P. Purushotham, K. Suma, K. Manjeet, S. Rambabu, N. E. El Gueddari, B. M. Moerschbacher, A. R. Podile. *Crit. Rev. Biotechnol*. **35**, 29 (2015).
[8] P. Miretzky, A. F. Cirelli. *J. Hazard. Mater*. **167**, 10 (2009).
[9] B. M. Moerschbacher, F. Bernard, N. E. El Gueddari. *Adv. Chitin Sci*. **XI**, 185 (2011).
[10] H. Kauss, W. Jeblick, A. Domard. *Planta* **178**, 385 (1989).
[11] P. Vander, K. M. Vårum, A. Domard, N. Eddine El Gueddari, B. M. Moerschbacher. *Plant Physiol*. **118**, 1353 (1998).
[12] A. L. W. dos Santos, N. E. El Gueddari, S. Trombotto, B. M. Moerschbacher. *Biomacromolecules* **9**, 3411 (2008).
[13] C. Chatelet, O. Damour, A. Domard. *Biomaterials* **22**, 261 (2001).
[14] J. Kumirska, M. X. Weinhold, J. Thöming, P. Stepnowski. *Polymers (Basel)*. **3**, 1875 (2011).
[15] C. Gorzelanny, B. Pöppelmann, K. Pappelbaum, B. M. Moerschbacher, S. W. Schneider. *Biomaterials* **31**, 8556 (2010).
[16] S. Cord-Landwehr, R. L. J. Melcher, S. Kolkenbrock, B. M. Moerschbacher. *Sci. Rep*. **6**, 38018 (2016).
[17] V. K. Mourya, N. N. Inamdar, Y. M. Choudhari. *Polym. Sci. Ser*. A **53**, 583 (2011).
[18] S. Popa-Nita, J.-M. Lucas, C. Ladavière, L. David, A. Domard. *Biomacromolecules* **10**, 1203 (2009).
[19] S. Trombotto, C. Ladavière, F. Delolme, A. Domard. *Biomacromolecules* **9**, 1731 (2008).
[20] M. Abla, L. Marmuse, F. Delolme, J.-P. Vors, C. Ladavière, S. Trombotto. *Carbohydr. Polym*. **98**, 770 (2013).
[21] N. Barroca-Aubry, A. Pernet-Poil-Chevrier, A. Domard, S. Trombotto. *Carbohydr. Res*. **345**, 1685 (2010).
[22] Y. Yang, B. Yu. *Tetrahedron* **70**, 1023 (2014).
[23] Y. Zhao, R. D. Park, R. A. A. Muzzarelli. *Mar. Drugs* **8**, 24 (2010).
[24] W. J. Jung, R. D. Park. *Mar. Drugs* **12**, 5328 (2014).
[25] S. N. Hamer, S. Cord-Landwehr, X. Biarnés, A. Planas, H. Waegeman, B. M. Moerschbacher, S. Kolkenbrock. *Sci. Rep*. **5**, 8716 (2015).
[26] K. Tokuyasu, H. Ono, M. Ohnishi-Kameyama, K. Hayashi, Y. Mori. *Carbohydr. Res*. **303**, 353 (1997).
[27] X. Li, L.-X. Wang, X. Wang, S. Roseman. *Glycobiology* **17**, 1377 (2007).
[28] R. Chambon, G. Despras, A. Brossay, B. Vauzeilles, D. Urban, J.-M. Beau, S. Armand, S. Cottaz, S. Fort. *Green Chem*. **17**, 3923 (2015).
[29] S. Haebel, S. Bahrke, M. G. Peter. *Anal. Chem*. **79**, 5557 (2007).
[30] F. Henning Cederkvist, M. P. Parmer, K. M. Vårum, V. G. H. Eijsink, M. Sørlie. *Carbohydr. Polym*. **74**, 41 (2008).
[31] S. Naqvi, S. Cord-Landwehr, R. Singh, F. Bernard, S. Kolkenbrock, N. E. El Gueddari, B. M. Moerschbacher. *Appl. Environ. Microbiol*. **82**, 6645 (2016).

[32] A. Varki, R. D. Cummings, M. Aebi, N. H. Packer, P. H. Seeberger, J. D. Esko, P. Stanley, G. Hart, A. Darvill, T. Kinoshita, J. J. Prestegard, R. L. Schnaar, H. H. Freeze, J. D. Marth, C. R. Bertozzi, M. E. Etzler, M. Frank, J. F. Vliegenthart, T. Lütteke, S. Perez, E. Bolton, P. Rudd, J. Paulson, M. Kanehisa, P. Toukach, K. F. Aoki-Kinoshita, A. Dell, H. Narimatsu, W. York, N. Taniguchi, S. Kornfeld. *Glycobiology* **25**, 1323 (2015).
[33] B. Domon, C. E. Costello. *Glycoconj. J.* **5**, 397 (1988).